Metastable-state dynamics of a liquid: A free-energy landscape study

Bhaskar Sen Gupta, Leishangthem Premkumar, and Shankar P. Das

School of Physical Sciences, Jawaharlal Nehru University, New Delhi 110067, India

Using the time dependence of density fluctuations in a supercooled liquid obtained from the solutions of the equations of nonlinear fluctuating hydrodynamics (NFH), the evolution of the system in the free energy landscape is studied. A crossover from a continuous fluid type dynamics to that of hopping between different free energy minima is observed as the liquid is increasingly supercooled. We demonstrate that our results are also in agreement with equilibrium density functional analysis of the same system. The density field obtained in the numerical solution of the NFH equations are further analyzed to introduce complimentary density of voids in the supercooled liquid state and its static and dynamic correlations are computed. The nature of the relaxation of vacancy correlations are observed to be similar to that of the density fluctuations.

I. INTRODUCTION

Landscape studies of many particle systems have been an area of much research interest. In particular, the potential energy landscape studies have been widely applied for various disciplines of chemical physics [1], ranging from clusters, glassy systems, to proteins. In 1969, in a seminal paper Goldstein [2] presented a picture for the dynamics of the supercooled liquid based on the evolution of the system in the multidimensional phase space of all its configurational degrees of freedom. In a simple monoatomic system of N particles in three dimensions this refers to a set of total $3N$ coordinates. The total potential energy $U(\mathbf{r}_1, \ldots, \mathbf{r}_N)$ of the system defines a hypersurface termed as the potential energy landscape (PEL). It is characterized by different minima of the potential energy among which the local ones represent the amorphous structures. Below the freezing point T_m the crystalline state with long range order corresponds to lowest free energy. The PEL is related to the mechanical property of the N particle system and is not dependent on the temperature T, which refers to the thermodynamic state of the system. However, the part of the landscape explored by the system is strongly dependent on the temperature. At a finite temperature there are fluctuations of the energy which allow the system, represented by a single point moving over the PEL, to move from one minimum to another through barrier crossing. For the equilibrium liquid which is ergodic, these jumps occur between minima which have similar energy values on the average. At low temperature the point representing the system remains confined to a local minimum until it moves out by making activated jumps over potential barriers. The atoms are localized having small vibrations around positions on an amorphous lattice structure. In terms of the PEL this situation is described as the single representative point for the system making small (vibrational) motions around a local minimum of the potential energy in the $(3N + 1)$ dimensional space. This state continues until a large enough fluctuation causes the system to jump over the potential barrier to move to another minimum. This activated barrier hopping in the PEL for the supercooled liquid was interpreted by Goldstein as a rearrangement of particles in a small region of the system in the real space. Such rearrangements can occur independently in different parts of the system at low temperature.

While the PEL paradigm discussed above has been widely applied for studying the supercooled liquids, a similar approach in terms of the free energy is somewhat less explored. The equilibrium state of a many particle system at a finite temperature is controlled by its free energy reaching a minimum. For studying the glassy state this concept of equilibrium free energy is often generalized to a coarse grained free energy functional expressed in terms of a set of suitable order parameters. In the density functional theory which has been widely applied for studying equilibrium phase transitions [3–5], the free energy is treated as a functional of the density.

The most obvious choice of the parameters for the coarse grained free energy of a system with heterogeneous density profiles is a set of spatial coordinates $\{\mathbf{R}_i\}$. The latter corresponds to the centers of the inhomogeneous density profiles $\rho(\mathbf{r})$ in the system. In other words, $\{\mathbf{R}_i\}$'s denote the average positions of the constituent particles in a localized state. Such a parametrization defines a multidimensional landscape. With the entropic contribution included this is generally referred to as the free energy landscape (FEL). Models for the supercooled liquids have been studied by evaluating the free energy functional for a small number of particles. The size of the system considered is smaller and is similar to the molecular dynamic simulations with a finite size system in which the periodic boundary conditions are used. The structure of the FEL is crucially linked to the choice of a suitable functional in terms of the density function. The free energy of the metastable liquid is obtained by minimizing a functional corresponding to the optimum choice of the inhomogeneous density function [6,7]. In the standard formulation of the density functional theory, the free energy functional is given by

$$F[\rho] = \int d\mathbf{r}\rho(\mathbf{r})[\ln(\rho(\mathbf{r})/\rho_0) - 1] + F_{\text{in}}, \qquad (1)$$

where the first term is the ideal gas entropy contribution and the second term is the interaction part F_{in} obtained to a quadratic order in density fluctuations as

$$\beta F_{\text{in}} = -\frac{1}{2m^2} \int d\mathbf{r} d\mathbf{r}' c(\mathbf{r} - \mathbf{r}') \delta\rho(\mathbf{r}) \delta\rho(\mathbf{r}'), \qquad (2)$$

where $c(r)$ is the two point Ornstein-Zernike direct correlation function [8] and m is the mass of the particles in the one component fluid. The optimization of the above form referred to as the Ramakrishnan-Yussouff free energy functional with respect to aperiodic density profiles was done numerically [9] in the supercooled regime. Similar approaches were used [10–12] for evaluating the equilibrium free energy $F[\rho]$ of the amorphous solidlike state by parameterizing the density in terms of a small number of Gaussian density profiles localized around a set of points $\{R_i\}$ which are treated as free parameters in the model. Monte Carlo dynamics was used [13] to obtain the density fluctuations and study the above free energy functional in order to study the evolution of the metastable state. The dynamics was also studied with a discretized version of the Fokker-Planck equation in the form of a mesoscopic kinetic equation [14,15]. This involved mapping the problem to a kinetic lattice gas type model in which the system is divided into an assembly of primitive cells and the local density is treated as the only relevant variable.

In the present work we consider the dynamics of the metastable liquid in terms of its evolution in the FEL. The free energy functional given by Eq. (2) is evaluated in terms of the corresponding density fluctuations obtained from the direct solutions of the equations of the nonlinear fluctuating hydrodynamics (NFH). These equations describe the dynamics of conserved or slow variables, namely mass, momentum, and energy density. The physical significance of the fluctuating hydrodynamics approach to the glassy relaxation is that the correlated motion of the particles is expressed through the nonlinear coupling of the slow modes. The latter becomes very important in describing the strongly correlated liquid dynamics in the dense supercooled state. The NFH equations mainly contain two parts: the reversible part which includes the coupling of slow modes and the stochastic part representing the thermal noise in the system. In our earlier work we studied extensively the equilibrium and nonequilibrium dynamics [16,17] of the supercooled liquid from the direct numerical solutions of the NFH equations. These equations provide a reliable way of studying the dynamics of fluctuations in a dense liquids. In the present work we study how a one component dense liquid explores the corresponding FEL. We also study the nature of the frozen state from an analysis of the density profiles obtained as the solutions of the NFH equations. In particular, we use the density profiles in the amorphous state to study the dynamics of voids in the metastable structures and compare the associated time scales with the corresponding times for relaxation of density fluctuations.

In the next section we introduce the model used for obtaining the density fluctuations from the numerical solution of the equations of NFH. In Sec. III we describe the evolution of the system in terms of the dynamics in the FEL. We also present in this section an analysis using the equilibrium density functional approach and compare the findings with those from the dynamical solutions. Following this we study the crossover nature of this dynamics by introducing a state vector $|\Psi^\nu(t)\rangle$ for a particular state labeled as ν at time t, by representing all the densities at the lattice points at t. We use this state vector to study the nature of the system's dynamics in FEL. In Sec. IV we analyze the dense metastable structures of the liquid to introduce a characteristic vacancy density for the supercooled

liquid and study its static and dynamic correlations. We end the paper with a discussion of the results.

II. THE MODEL FOR DYNAMICS

A. The generalized Langevin equations

The equations of NFH for a set of slow modes $\{\phi_i\}$ are obtained in the form [18]

$$\frac{\partial \phi_i(t)}{\partial t} = V_i[\phi] + \sum_j \left[\beta^{-1} \frac{\partial L_{ij}^0(\phi)}{\partial \phi_j} - L_{ij}^0 \frac{\partial F}{\partial \phi_j} \right] + \theta_i(t),$$
(3)

where V_i is the reversible part of the dynamics and L_{ij}^0 represents bare transport matrix in the dissipative term and is equal to correlation of the noise θ_i assumed to be white and Gaussian. V_i is expressed in terms of Poisson brackets Q_{ij} of the slow variables $\{\hat{\phi}_i\}$ (the hat indicates the microscopic variable dependent on phase space coordinates) and the functional $F[\phi]$ which is identified with the free energy functional determining the equilibrium state of the system (see below).

For the case of compressible liquid explicit calculation obtains from the above formulation, respectively, the continuity equations of the mass density ρ and momentum density **g**,

$$\frac{\partial \rho}{\partial t} + \nabla \cdot \mathbf{g} = 0,$$
(4)

and that for **g** is the generalized nonlinear Navier-Stokes equation [19],

$$\frac{\partial g_i}{\partial t} + \nabla_j \left[\frac{g_i g_j}{\rho} \right] + \rho \nabla_i \frac{\delta F}{\delta \rho} + L_{ij} \frac{g_j}{\rho} = \theta_i.$$
(5)

where $F[\rho]$ is the solely density dependent part of the effective Hamiltonian and is defined by the Eq. (1) above. For an isotropic liquid the Gaussian noise θ_i is related to the bare damping matrix L_{ij} [8] as

$$\langle \theta_i(x,t)\theta_j(x't') \rangle = 2k_B T L_{ij}\delta(t - t')\delta(x - x'),$$
(6)

where

$$L_{ij} = (\zeta_0 + \eta_0/3)\delta_{ij}\nabla^2 + \eta_0 \nabla_i \nabla_j.$$
(7)

Here ζ_0 and η_0 represent the bare bulk and shear viscosities, respectively. We work here with the set of variables containing density and momentum density and solve these equations numerically to obtain the density fields on a grid of cubic lattice.

The probability $P[\phi,t]$ that the collective modes $\{\phi_i\}$ have the value $\{\phi_i\}$ at time t, where $\phi \equiv \{\rho, \mathbf{g}\}$ is controlled by the Fokker-Planck equation corresponding to the above generalized Langevin equations,

$$\frac{\partial}{\partial t} P[\phi,t] = \mathcal{D}_\phi P[\phi,t],$$
(8)

with $\mathcal{D}_\phi$ as the corresponding driving operator,

$$\mathcal{D}_\phi = -\sum_i \frac{\partial}{\partial \phi_i} \left[V_i[\phi] - \beta^{-1} \sum_j L_{ij}^0(\phi) \left(\frac{\partial}{\partial \phi_j} + \beta \frac{\partial F[\phi]}{\partial \phi_j} \right) \right].$$
(9)

The $V_i[\phi]$ represent the reversible part of the Langevin equation (3) for the slow mode ϕ_i and satisfy the divergence condition

$$\sum_i \frac{\partial}{\partial \phi_i}\{V_i(\phi)P[\phi]\} = 0. \tag{10}$$

The probability of the equilibrium state $P[\phi,t]$ does not have any explicit time dependence such that $\mathcal{D}_\phi P_{EQ}[\phi] = 0$. Using (10) it is straightforward to show that $\exp\{-F[\phi]\}$ is a stationary solution of the Fokker-Planck equation. In the present formulation $F[\rho, g_i] = F_K[\rho, g] + F[\rho]$ is a functional of both mass density ρ as well as momentum density $\mathbf{g}$. However, the Gaussian dependence of the dependence on $\mathbf{g}$ in $F_K[\rho, g]$ is integrated out and in the following we focus on the functional $F[\rho]$ of density only. In doing this we ignore the presence of a counterterm $\ln[\rho/\rho_0]$ [20] due to the $1/\rho$ nonlinearity in the kinetic energy term F_K. The primary motivation here is to focus on the dynamics of slowly decaying density fluctuations in the supercooled state.

B. Numerical solution of NFH equations

We consider the one component liquid of N particles interacting via Lennard-Jones (LJ) potential,

$$u(r) = 4\epsilon[(\sigma/r)^{12} - (\sigma/r)^6]. \tag{11}$$

The units of different variables are chosen so as to make subsequent expressions dimensionless. In our model there are two length scales: One is the length scale σ associated with the LJ potential and the other is the length h of the lattice grid on which ρ and $\mathbf{g}$ are computed. We choose the ratio of these length scales to be incommensurate, that is, $\sigma/h = 4.6$. Time and length are respectively scaled with the LJ unit of $\tau_0 = (m\sigma^2/\epsilon)^{\frac{1}{2}}$ and the grid size h. The thermodynamic state of the fluid is described in terms of the reduced density $\rho_0^* = \rho_0 \sigma^3$ and the reduced $T^* = (k_B T)/\epsilon$. Here ρ_0 represents the total number of particles per unit volume and T is the temperature. To keep notations simple we choose the mass m of the particles to be unity so that the number and mass densities are same. The local density $\rho(\mathbf{x},t)$ and momentum density $\mathbf{g}(\mathbf{x},t)$ are respectively chosen in terms of dimensionless quantities

$$n(\mathbf{r}) = [h^3 m^{-1}]\rho(\mathbf{r}), \tag{12}$$

$$\mathbf{j}(\mathbf{r}) = \left[h^3(m\epsilon)^{-\frac{1}{2}}\right]\mathbf{g}(\mathbf{r}). \tag{13}$$

The speed of sound c_0 is given by, $c_0^2 = k_B T/[mS(0)]$. We study the time evolution of the system in terms of that of the free energy functional $F[\rho]$. In the standard density functional theory, which is a thermodynamic approach, minimum value of this functional is searched in the multidimensional parameter space of density. In the present work we evaluate the free energy functional as the density profiles $\rho(\mathbf{x},t)$ evolves in time. The density field is obtained from the numerical Eqs. (4) and (5) on a three dimensional cubic lattice.

The details of the numerical solution of the nonlinear fluctuating hydrodynamic equations have been discussed in Ref. [16]. We list here two important features. First, the third term of Eq. (5) representing a nonlocal contribution is calculated by dividing the cubic grid into concentric spherical shells and evaluating the nonlocal integral $f(r,t)$ as a sum

of contributions from the successive shells. Second, a major concern in solving the nonlinear stochastic equations is the stability of the numerical algorithm. In the earlier work [21] for a similar model the stability was maintained by violating the fluctuation dissipation theorem. We also encounter a similar problem in the numerical solution of our model. Due to the presence of the Gaussian noise $n(\mathbf{x},t)$ gets negative at certain grid points. To overcome this problem we adopt the following coarse graining scheme also outlined in Ref. [16]. The positivity of the density field $n(\mathbf{x},t)$ over the whole grid is maintained at each time step during the evolution of our system. With this scheme we have successfully avoided the numerical instability and solve the nonlinear equation for long time where fluctuation dissipation relation is respected.

III. FREE ENERGY LANDSCAPE DESCRIPTION

A. Dynamics of density fluctuations

For studying the dynamics of a dense liquid, we analyze the free energy $F[\rho]$ of the density field $\rho(\mathbf{x},t)$. The change in the free energy of the inhomogeneous state from that of the uniform state is obtained as

$$\Delta F[\rho] = \beta F[\rho] - \beta F_l[\rho_0] = \int d\mathbf{r}[\rho(\mathbf{r})\ln(\rho(\mathbf{r})/\rho_0) - \delta\rho]$$

$$- \frac{1}{2m^2}\int d\mathbf{r}d\mathbf{r}'\, c(\mathbf{r} - \mathbf{r}')\delta\rho(\mathbf{r})\delta\rho(\mathbf{r}'), \tag{14}$$

where $F[\rho]$ is the total free energy of the inhomogeneous liquid and F_l is that of a uniform liquid of density ρ_0. We compute the functional $\Delta F[\rho(\mathbf{x},t)]$ at each time step in terms of the density fluctuations to study the dynamical evolution of our system in the PEL. The fluctuating density field $\rho(\mathbf{x},t)$ is obtained from the solution of the equations of NFH over the cubic grid and is stored in suitably chosen time bins. This study is done at five different temperatures $T = 0.4$, 0.6, 0.8, 1.0, and 1.2 at constant density $n^* = 1.10$. For each temperature the density fields is computed on a cubic grid of size h having $\mathcal{S} \times \mathcal{S} \times \mathcal{S}$ points. Periodic boundary condition is maintained. This essentially means a system of $\rho_0^*(\mathcal{S}\kappa)^3 = \mathcal{N}(say)$ particles in the box of volume $V = (\mathcal{S}h)^3$, where $\kappa = h/\sigma$ is the ratio of the two characteristic length scales. κ is chosen to be incommensurate, that is, $\sigma/h = 4.6$. For the available computation strength we take the cubic box of size $\mathcal{S} = 20$. At each temperature the free energy per particle $f[\rho] = \Delta F[\rho]/\mathcal{N}$.

Equilibration of the liquid around a stable or metastable state is inferred when the free energy $f[\rho]$ fluctuates around a steady value which signifies a minimum in the FEL. In this we observe two qualitatively different types of behavior in the time evolution of the free energy functional.

(A) For higher temperatures, in the range 0.8–1.2, over long times the $F[\rho]$ settles around a single average value. In Fig. 1 we show that for $T = 0.8$, $f[\rho] \sim 0 (\equiv F[\rho]/N)$, that is, the system is in the global free energy minimum or in liquid state. For somewhat higher temperatures $T = 1.0$ and 1.2 (until below the crystallization point T_m) the average over which the free energy $f[\rho]$ fluctuates is slightly higher than that of the uniform liquid state. This indicates that at this high T the system stays in the metastable state with
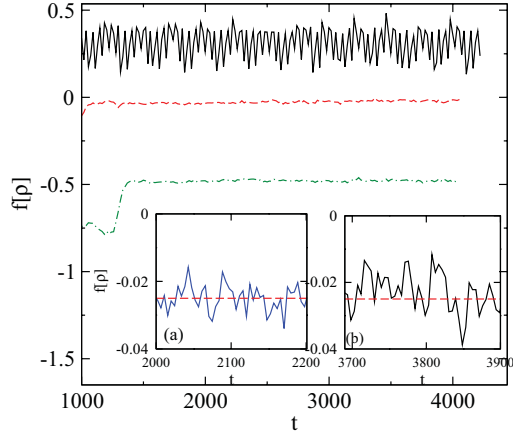
FIG. 1. (Color online) $f[\rho]$ (in units of β^{-1}) vs t/τ_0 at $n^* = 1.10$ and $T^* = 1.0$ (solid line), 0.8 (dashed line), 0.6 (dot-dashed line). The inset shows the $T^* = 0.8$ results with higher magnifications over two different time windows respectively in (a) and (b).

higher $f[\rho]$ over this time scale of observation. Eventually, the metastable liquid should crystallize going to the most stable state corresponding to the temperature ($<T_m$). As the liquid is further supercooled the free energy corresponding to the metastable state goes below that of the uniform liquid. The average $f[\rho]$ becomes negative with decrease in T, indicating that at this temperature the supercooled metastable state has a lower free energy than the uniform liquid state. Beyond this temperature the metastable glassy state is more stable than the uniform liquid state.

(B) At low temperatures we observe a qualitative change in the nature of time evolution of the free energy density. Unlike the high temperature case, here the free energy functional does not settle at some average value in the long time limit. Over the different time windows, the free energy remains close to some average value until making a jump beyond which it fluctuates around a different average value. This behavior is displayed in Fig. 2.
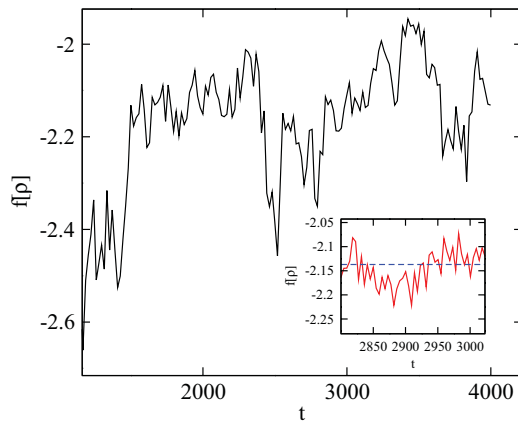

FIG. 2. (Color online) $f[\rho]$ (in units of β^{-1}) vs t/τ_0 at $T^* = 0.4$ and $n^* = 1.10$ for large times. The inset shows the results over shorter time windows with higher magnification. The dashed line is the mean value of free energy over this time window.
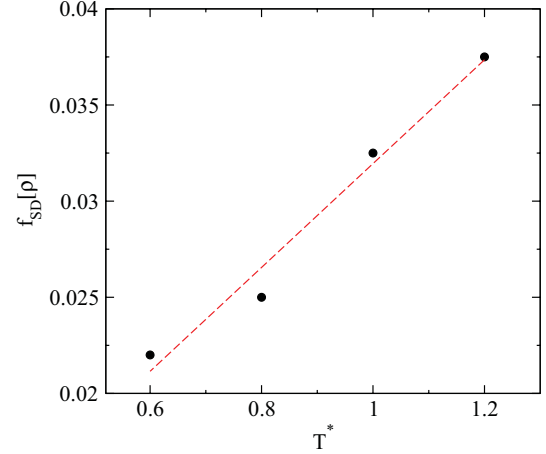

FIG. 3. (Color online) Standard deviation of the free energy $f_{SD}[\rho]$ (in units of β^{-1}) vs T^* graph at $n^* = 1.10$ is presented by solid points. The dashed curve is the straight line fit.

In both Figs. 1 and 2, in the respective insets we display the fluctuations of the free energy around the corresponding minimum over the selected time window. Average of these fluctuations represented by the standard deviation of the free energy within the respective window is taken as a measure of the vibrational contribution. This excess harmonic part is plotted in Fig. 3 with temperature displaying the expected linear behavior.

B. Density functional model

The above observations of the dynamics of the system in terms of the evolution in the FEL are obtained from the direct solutions of the equations of motion for the density. These results are further consolidated with a complementary calculation of minimizing the free energy in the equilibrium density functional approach [7,12,22]. The density functional theory evaluates the free energy $F[\rho]$ of the solid state as a functional of the corresponding inhomogeneous density function $\rho(\mathbf{x})$ for the equilibrium state. The free energy $F[\rho]$ is expanded around that of the corresponding uniform liquid of constant density ρ_0 in terms of functional Taylor expansion. The coefficients of the expansion are the successive functional derivatives of F with respect to $\rho(\mathbf{x})$ evaluated at uniform density ρ_0. At second order this is the two point direct correlation function $c(r)$ for the uniform state and is a required input in the theory. In addition, details of the structure of the solid state constitute another input needed in the DFT to describe the inhomogeneous density of the solid. Generally the density function is defined in terms of a sum of Gaussian profiles centered around a set of fixed lattice points. In case of the fcc crystal these are the points on a fcc lattice with long range order. For the amorphous solid we use here the Bernal structure [23] which represents in terms of the corresponding pair function $g_B(r)$ the structure of the random lattice points on which the Gaussian density profiles are centered.

In order to evaluate the free energy functional described in Eqs. (1) and (2) the inhomogeneous density function $\rho(\mathbf{x})$ is expressed as the superposition of Gaussian density profiles

centered on a lattice,

$$\rho(\mathbf{r}) = \sum_i \phi(|\mathbf{r} - \mathbf{R}_i|), \qquad (15)$$

where the $\{\mathbf{R}_i\}$ denotes the underlying lattice sites. The function ϕ is taken as the isotropic Gaussian,

$$\phi(r) = \left(\frac{\alpha}{\pi}\right)^{\frac{3}{2}} e^{-\alpha r^2}.$$

The input required in this calculation is the distribution of centers for the Gaussian density profiles. In case of a crystalline structure it is the corresponding lattice with long range order. The width of the Gaussian profiles are given by the inverse of the parameter $\sqrt{\alpha}$. The range $\alpha\sigma^2 \gg 1$ corresponds to the highly localized structure. In this range the ideal gas part of free energy per particle is approximated to its asymptotic value for large α,

$$\beta f_{\text{id}}[\rho] = -\frac{5}{2} + \ln\left[\Lambda^3 \left(\frac{\alpha}{\pi}\right)^{\frac{3}{2}}\right].$$

In the low α region the overlapping Gaussians from different sites contribute and we account for such density profiles. The ideal gas part in this case is expressed as

$$\beta f_{\text{id}}[\rho] = \int d\mathbf{r}\phi(\mathbf{r})\Bigg\{\ln\Bigg[\Lambda^3 \int d\mathbf{R}\phi(\mathbf{r}-\mathbf{R})(\delta(\mathbf{R})$$
$$+ \rho_0 g(\mathbf{R}))\Bigg] - 1\Bigg\}, \qquad (16)$$

where $g(\mathbf{R})$ is the site-site correlation function in terms of which the random structure is parameterized. We approximate the pair correlation function in terms of the isotropic function [24,25] $g(R)$, which is defined in the parametric form

$$g(R) = g_B\left[R\left(\frac{\eta}{\eta_{RCP}}\right)^{\frac{1}{3}}\right], \qquad (17)$$

where $g_B(r)$ is the structure corresponding to the Bernal random packing obtained using Bennett algorithm [26]. Increasing η_{RCP} in the expression maps to a system with increasingly separated or loose underlying lattice structure. For $\eta = \eta_{RCP}$ the structure corresponds to Bernal packing for which the pair correlation is displayed in Fig. 4. The other input in this density functional calculation is the direct correlation function $c(r)$ appearing in the interaction part of the free energy functional in Eq. (2). The $c(r)$ corresponding to the uniform liquid state at supercooled temperature is approximated using the Bridge function method of Due and Haymet [27]. The different $c(r)$ values used in the calculation at different temperatures are shown as an inset in Fig. 5.

The free energy difference as defined in Eq. (2) and computed using the Bernal structure function is plotted with width parameter α in Fig. 6. Here this is displayed for different values of temperatures T^* at constant density of $\rho_0^* = 1.1$. For each of the temperatures studied, a free energy minimum occurs at an intermediate α value and predicts the existence of a metastable state. These density profiles for these intermediate α values are far less localized than the usual crystalline state ($\alpha\sigma^2 \sim 100$). However the heterogeneous state is very different from the uniform liquid state corresponding to
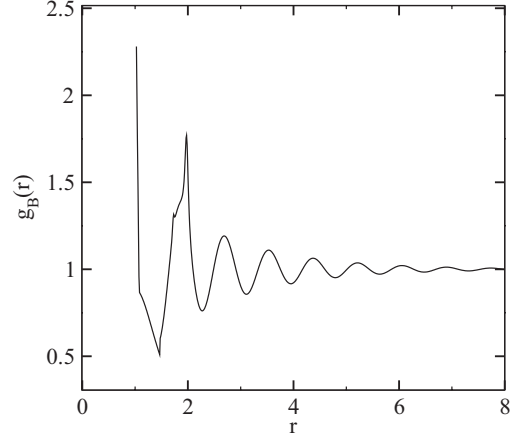
FIG. 4. The Bernal $g_B(r)$ used in choosing the distribution of the Gaussian centers of overlapping Gaussian profiles.

($\alpha\sigma^2 \to 0$). For $T > 0.8$ this finite α state is relatively less stable than the uniform liquid state and has a higher free energy. With increased supercooling the metastable state becomes more stable than the uniform liquid state. This is dependent on the amorphous structure associated with the inhomogeneous state controlled by the parameter η_{RCP}. The origin of the Gaussian density profiles lies on a random structure characterized in terms of the pair correlation function corresponding to the parameter value $\eta_{RCP} = 0.671$ in Eq. (17).

The metastable states obtained in the density functional calculation is in agreement with our findings in the previous section using a dynamic approach with the solutions of the NFH equations. The difference Δf between the free energies (scaled with respect to β^{-1}) of the metastable state and the uniform liquid state obtained, respectively, from the DFT and NFH calculations are displayed in Table I. The behaviors seen from the two types of theories are qualitatively in agreement.

C. Evolution of the supercooled state

In order to investigate thermally activated transitions among the free energy minima we now introduce a state vector
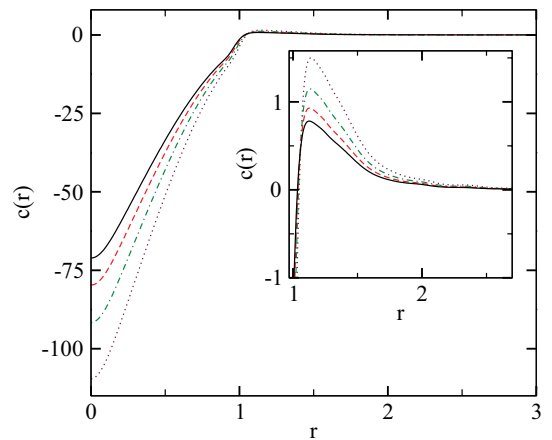
FIG. 5. (Color online) Direct correlation function $c(r)$ vs r/σ at $\rho_0^* = 1.1$ and $T^* = 1.2$ (solid line), 1.0 (dashed line), 0.8 (dot-dashed line), and 0.6 (dotted line) using the bridge function method [27].
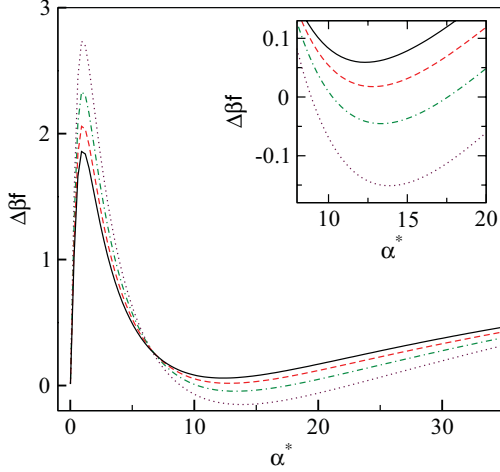
FIG. 6. (Color online) The free energy difference (in units of β^{-1} vs width parameter $\alpha\sigma^2$ at $\rho_0^* = 1.1$ and $T^* = 1.2$ (solid line), 1.0 (dashed line), 0.8 (dot-dashed line), and 0.6 (dotted line) for the LJ system.

involving the densities at all the $\mathcal{N}$ points in the cubic lattice. The vector $|\Psi^\nu(t)\rangle$ characterizing the state (labeled as ν) of the system is defined in terms of set of basic vectors $|e_i\rangle$ as follows:

$$|\Psi^\nu(t)\rangle = \sum_{i=1}^{\mathcal{N}} n_i^\nu(t)|e_i\rangle, \tag{18}$$

where $n_i^\nu(t)$ is the scaled density at the lattice site i and is defined as $n_i^{nu}(t) = \rho(\mathbf{R}_i)\sigma^3$, where $\mathbf{R}_i$ denotes the ith lattice site for the state ν. The set of numbers $\{n_i^\nu(t)\}$ satisfies the constraint $\mathcal{N}^{-1}\sum_i n_i^\nu(t) = \rho_0^* \equiv \rho_0\sigma^3$. The basic vectors $|e_i\rangle$'s, defined as

$$|e_i\rangle = |0\dots0.\underbrace{1}_{i}.0\dots0\rangle, \tag{19}$$

represent the ith orthonormal basis(of size $\mathcal{N}$) in the corresponding vector space. The superscript ν in $|\Psi^\nu(t)\rangle$ refers to a particular initial state. At a given time this vector represents the state of the system. In order to study how the system explores in the FEL, we study the overlap of the $|\Psi^\nu(t)\rangle$ at two different times. To quantify this overlap we define the overlap function $q(t)$ as

$$q(t) = \frac{\langle\Psi^\nu(t)|\Psi^\nu(0)\rangle}{\langle\Psi^\nu(0)|\Psi^\nu(0)\rangle}, \tag{20}$$

where the averaging is implied over a set of chosen initial states ν and $\langle\cdots|\cdots\rangle$ denotes taking a scalar product of the

TABLE I. The free energy differences in units of β^{-1} at $\rho_0\sigma^3 = 1.1$ and different temperature T^* from the dynamic approach and density functional approach.

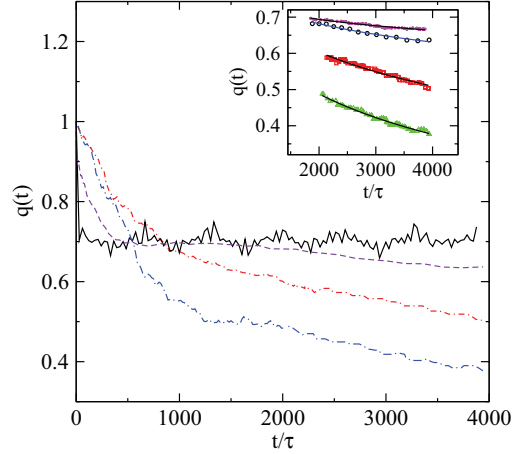| T	Thermodynamic (DFT)	Dyanmic (FNH)
1.0	0.16	0.3
0.8	-0.04	-0.04
0.6	-0.15	-0.5

FIG. 7. (Color online) Order parameter $q(t)$ [see text] as a function of t/τ_0 for $n^* = 0.9$ and $T^* = 1.2$ (solid line), $n^* = 1.1$ and $T^* = 0.8$ (dashed line), 0.6 (short dash-dotted line), and 0.4 (long dash-dotted line). In the inset we show the $q(t)$ for large t/τ_0 at $T^* = 1.0$ (stars), 0.8 (circles), 0.6 (squares), and 0.4 (triangles) fitted with KWW form (solid line).

two vectors. The definition of the overlap function $q(t)$ ensures that it is normalized to have value unity at $t = 0$.

Using directly the density field $\rho(\mathbf{x},t)$ obtained in the numerical solution of the NFH equations the correlation functions $q(t)$ is computed. If the system remains near the same free energy minimum, this is indicated in a slow decay of the correlation $q(t)$. The hopping of the system from one minimum to another is signaled by a quicker decay of $q(t)$ which therefore displays a faster relaxation at lower temperatures. In Fig. 7 we show the time evolution of $q(t)$ for different density and temperature regimes. In the normal liquid state ($n^* = 0.9, T = 1.2$) the correlation $q(t)$ freezes at a constant value over long times or decays very slowly over observed time scales. At higher temperature the correlation persists for longer time, indicating that the liquid remains confined to a single thermodynamic state. Simple fitting shows that $\tilde{\tau}$ grows as a power law $(T_c' - T)^{-a'}$ with $T_c' = 1.54$, which is higher than the corresponding freezing point T_m corresponding to a normal liquid state. Temperatures above T_c' signify liquidlike behavior. In the supercooled state ($n^* = 1.1, T = 0.6$), on the other hand, $q(t)$ does not remain constant and it decays with time, indicating reduced overlap between the states at two different times. The correlation becomes weaker at higher densities, indicating that the system is no longer confined to a single minimum and wanders in the FEL. The long dash-dotted curve in Fig. 7 displays $q(t)$ at $T = 0.4$. A careful observation of the evolution of $q(t)$ at the low temperature reveals a two step process: Following an initial decay at short time, the correlation function stays on a plateau over an intermediate time window and eventually decays to zero over longer times. This intermediate time behavior indicates that the system remains trapped in one of the glassy minima of the free energy. It eventually relaxes to states with lower free energies via thermally activated hopping transitions over free energy barriers. The behavior of $q(t)$ signifies the activated hopping process. The long time part of $q(t)$ follows a stretched exponential relaxation $\exp[-(t/\tilde{\tau})^\beta]$.
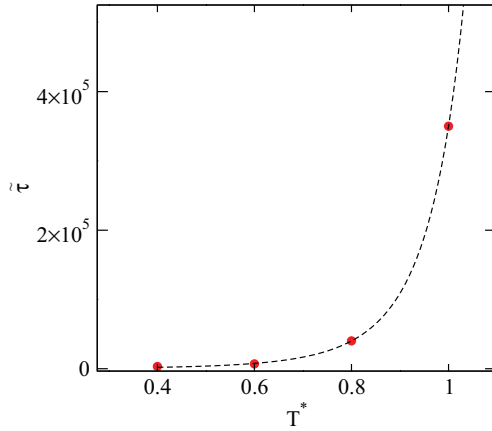
FIG. 8. (Color online) Variation of $\tilde{\tau}$ (see text) in LJ unit τ_0 as a function of T^*.

FIG. 9. (Color online) The number of vacant sites N_V vs t/τ_0 at $n^* = 1.10$ and $T^* = 0.8$. The corresponding result at $n^* = 1.10$ and $T^* = 0.6$ is shown in the inset.

The characteristic relaxation time $\tilde{\tau}$ is the time scale over which the system hops from one free energy minimum to other. The fitting to a stretched exponential form is shown in the inset of Fig. 7. The $\tilde{\tau}$ as a function of T^* is shown in Fig. 8. It increases with *increase* of T^*.

The results obtained above suggest the following scenario of the dynamics: At moderate supercooling the liquid largely fluctuates around a liquid state minimum. The relaxation time grows with increase of density. At this initial stage of supercooling the liquid state dynamics is still controlled by continuous fluid type motion of the particles. As the temperature falls beyond a crossover value, the dynamics is controlled by thermally activated hopping of the system in the FEL to configurations with inhomogeneous density distributions. In the low temperature state the system is caught in a local minimum of the free energy with only vibrational motion in the free energy basin. In real space this implies that the particles vibrate around their mean positions lying on disordered lattice structure. Dasgupta and Valls [13] in their study of the supercooled liquid dynamics in the FELs considered the RY functional expression [3] for the free energy. Here the density fluctuations were computed with Monte Carlo dynamics and the observed behavior is similar to what is depicted above. The time scale over which the system is moved to another adjacent free energy minimum is about three orders of magnitude higher than the corresponding microscopic time scale in the one component LJ system. While this is the typical scale of the slow dynamics for computer simulated supercooled liquids; it is much shorter than the very long activated process seen in experimental systems generally referred to in Goldstein's original PEL picture [2].

IV. VACANCY DENSITY AND SLOW DYNAMICS

The earlier sections of the paper consider the description of the supercooled liquid dynamics in the FEL paradigm. These are obtained here from a direct solution of the equations of NFH. In the present section we demonstrate how the same data is further analyzed for studying the dynamics of a new collective modes related to concentration of voids or free volumes in the supercooled liquid. The latter has often been
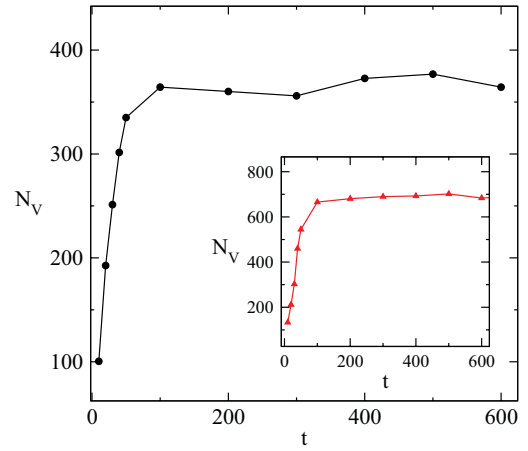
used in the literature for phenomenological models of glassy dynamics.

The numerical solution of the FNH equations obtains the fluctuating density fields $\rho(\mathbf{x}, t)$ over the cubic lattice and is saved at different times. Analyzing the fields it is observed that during the evolution of time at some of the grid points the densities become almost vanishing. We identify these points as vacancies or voids. To be more specific, we define vacancies as sites at which at a given time instant have reached a value less than 1% of the average density ρ_0. By studying the different profiles of the $n(\mathbf{x}, t)$ from the solutions of the NFH equations at different times, we observe that the location of the vacancies on the lattice are not stationary. They shift through the underlying lattice structure with time. Initially the number of vacant sites increases as the system evolves from the initial nonequilibrium state to a thermally equilibrated state and becomes steady varying with 10% of an average value at high density. The total number N_V, though not a strictly conserved quantity reaches a steady value. In the following we assume that the number of vacant sites remain constant on the average; that is, the average vacancy density ϱ_0 (say) remains constant at given thermodynamic state. ϱ_0 is strongly dependent on temperature and density. The vacancy density increases with decrease in temperature and increase in density. In Fig. 9 we show the number of vacant sites N_V as a function of time t at $n^* = 1.10$ for $T^* = 0.8$ and 0.6. In order to study the structural properties and the dynamics of these vacancies we assign the vacant sites with 1 and the rest of the sites (with nonzero density) as 0. Let us denote this new vacancy density field as $\varrho(\mathbf{x}, t)$, which is 1 or 0 depending on whether the lattice site is vacant or not, respectively.

We obtain corresponding to the density field $\varrho(\mathbf{x}_i) \equiv \varrho_i$ at the point $\mathbf{x}_i$ on the grid, the two point pair correlation function $\tilde{g}(r)$ using the following definition:

$$\tilde{g}(r) = \left\langle \frac{\Sigma_{i>j} \varrho_i \varrho_j f_{ij}}{\varrho_0^2 \Sigma_{i>j} f_{ij}} \right\rangle, \tag{21}$$

where the weight function $f_{ij} = 1$ if the separation between mesh points i and j lies between r and $r + \Delta r$ (Δr is a suitably chosen bin size), and $f_{ij} = 0$ otherwise. The angular
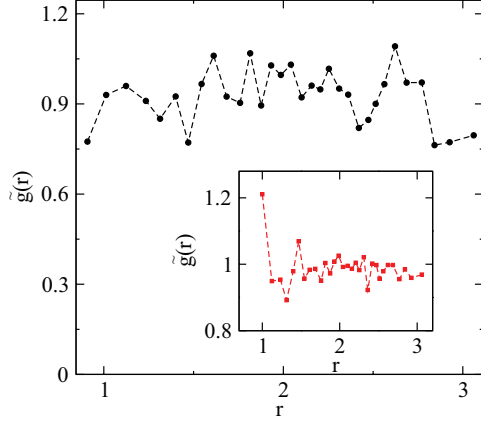
FIG. 10. (Color online) Pair correlation function $\tilde{g}(r)$ vs r (in units of σ) at $n^* = 0.97$ and $T^* = 2.0$ is shown in the main figure. The corresponding result at $n^* = 1.10$ and $T^* = 0.6$ is shown in the inset.

brackets refer to an average over the noise. The correlation function are computed after the time translational invariance has been attained indicating a thermally equilibrated state. The two equilibrium $\tilde{g}(r)$ vs r/σ plots displayed in Fig. 10 respectively correspond to two states, $T^* = 2.0$; $\rho_0^* = 0.97$ and $T^* = 0.6$; $\rho_0^* = 1.1$. At the lower density the average ϱ_0 is very low and $\tilde{g}(r)$ does not show much of a structure, indicating random occurrence of the vacant sites. At the higher density $\tilde{g}(r)$ has more oscillation around the average value 1. Next, the relaxation dynamics of the vacancy is studied in terms of the normalized time correlation function whose fourier transform at wave vector q is defined as

$$\tilde{\mathcal{C}}(q, t + t_{\rm w}, t_{\rm w}) = \frac{\langle \varrho(q, t + t_{\rm w})\varrho(-q, t_{\rm w})\rangle}{\langle \varrho(q, t_{\rm w})\varrho(-q, t_{\rm w})\rangle}. \quad (22)$$

At equilibrium, the $\tilde{\mathcal{C}}(q, t + t_{\rm w}, t_{\rm w})$ becomes a function of t only; for example, $\tilde{\mathcal{C}}(q, t + t_{\rm w}, t_{\rm w}) = \tilde{\mathcal{C}}(q, t)$. We calculate the correlation functions at the wave number $q = q_m$. The equilibrated system at density $\rho_0^* = 1.1$ for four temperatures $T^* = 1.0, 0.8, 0.7, 0.6$ is studied to obtain the $\tilde{\mathcal{C}}(t)$ as a function of time t and the result is displayed in Fig. 11. It is observed that unlike the correlation of density fluctuations the $\tilde{\mathcal{C}}(q,t)$ has a very weak wave vector dependence. This is presumably linked to the equal time structure factor having very weak wave vector dependence. The time correlation functions $\tilde{\mathcal{C}}(t)$ displays a stretched exponential relaxation. The corresponding relaxation time $\tilde{\tau}_\alpha$ and the stretching exponent $\tilde{\beta}$ at a given temperature are obtained by fitting a stretched exponential form (KWW) to the equilibrium correlation functions $\tilde{\mathcal{C}}(t)$. In Fig. 12 we show the variation of $\tilde{\tau}_\alpha$ as a function of T^*. In the same figure we show the τ_α calculated from the equilibrium number density correlation function of the occupied sites. These two relaxation processes are seen to be of similar nature and occurring over comparable time scales. The temperature dependence follows a power law growth $(T - T_c)^{-a}$ with a $T_c = 0.34$ and exponent $a = 2.62$. The corresponding exponent a from density correlation function data [16] with $T_c = 0.34$ is obtained as 2.22. The temperature dependence of the stretching exponent $\tilde{\beta}$ is shown in Fig. 13. The corresponding exponent β for the stretched exponential
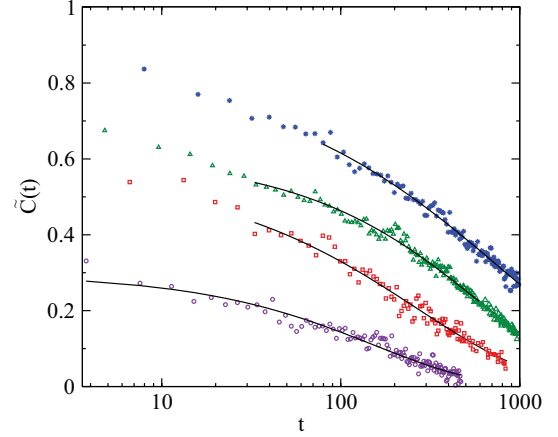

FIG. 11. (Color online) Equilibrated $\tilde{C}(t)$ vs t/τ_0 for temperature $T^* = 1.0$ (circles), 0.8 (squares), 0.7 (triangles), and 0.6 (stars) at $n^* = 1.10$. The solid lines are the best fit curves having the KWW form.

relaxation of the density correlation function is also displayed in the same figure. The stretching increases with the fall of temperature in both cases and is typical of slow dynamics.

V. DISCUSSION

From the evolution of the free energy functional computed using the solution of the NFH equations we note that at high temperature the system remains confined to single free energy minimum over the time scale studied. This inhomogeneous state corresponds to a metastable minimum of the free energy. With increase of supercooling the free energy of this state becomes less than that of the uniform liquid state. We also demonstrate here that this behavior is in agreement with results which follow from the equilibrium density functional theory calculation using the same free energy functional. The fluctuation of the free energy around the minimum value in the high temperature regime accounts for the vibrational
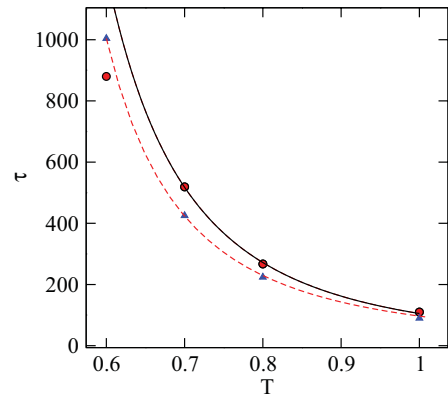

FIG. 12. (Color online) Relaxation time τ vs. temperature T expressed in Lennard Jones unit. The solid circles represent the relaxation time of vacancy auto correlation ($\tau \equiv \tilde{\tau}_\alpha$ in text) and solid triangles represent relaxation time for density auto correlation ($\tau \equiv \tau_\alpha$ in text). The points in each case are fitted with power-law forms shown respectively by solid and dashed lines.
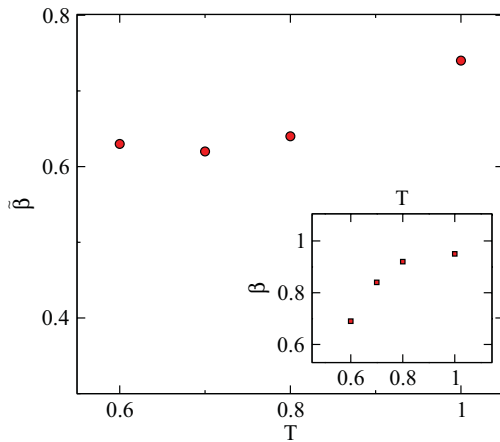
FIG. 13. (Color online) The stretching exponent $\tilde{\beta}$ vs T^* for the autocorrelations of vacancy (main figure) and density (inset).

contribution, which is shown to be linear in temperature dependence. At low temperature $T^* = 0.4$ the nature of the dynamics is qualitatively changed. The system, contrary to settling in one broad free energy basin at higher temperature with a single minimum, now hops between different basins representing highly inhomogeneous structures. It is important to note in this regard that what we are referring to as free energy is computed for a small number of particles in a finite size system. The free energy density is therefore an approximation of the thermodynamic quantity.

We have also investigated the nature of the inhomogeneous states into which the supercooled liquid evolves with time. For this the state representing the liquid at a given time is defined in terms of a single vector involving the densities at all the lattice sites as its components. The correlation between the state vectors at different times is defined in terms of the function $q(t)$. At high temperature, $q(t)$ freezes at a persistent value signifying very high overlap for long time. This indicates that the system is remaining near a single free energy minimum. However, at low temperatures $q(t)$ falls off much faster with time, showing that the deeply supercooled liquid is not remaining confined in a single free energy basin.

In Sec. III we describe the shifting of the representative point for the system in the multidimensional FEL from one minimum to another as a hopping process. In this regard it is useful to note that the same term hopping has been used in the literature for glassy dynamics in a somewhat different context. The latter refers to an interpretation of the ergodicity restoring mechanism in the mode coupling theory (MCT) for the glassy dynamics. In the simplest form of the MCT, the coupling of density fluctuations in the deeply supercooled liquid gives rise to a feedback mechanism and leads to an ergodic-nonergodic (ENE) transition. The autocorrelation of the density fluctuations slows down sharply approaching the mode coupling dynamic transition at a temperature T_c [28–30] which lies between freezing point and the calorimetric glass transition. A simple physical interpretation of this feedback process is that the nonlinear interaction of the density fluctuations signifies the cage effect for the single-particle motion. The above ENE transition of simple MCT signals the trapping of the single particle dynamics in the cage formed

by surrounding particles. It was subsequently demonstrated from a careful consideration of the equations of NFH that the $1/\rho$ nonlinearities present in these equations give rise to mechanisms for removal of this sharp transition [19,31]. These so called extended MCT models, however, assume expansions about a single fluid type minimum of the free energy. No activated process of hopping is involved between states of different free energy minima in reaching the cutoff mechanism. In some works [32,33], however, the ergodicity restoring mechanisms have been interpreted as the "hopping process" in the supercooled liquid, drawing a similarity between the dynamics of supercooled liquids with the transport process in strongly disordered semiconductors. A tagged particle motion in the latter is characterized by phonon assisted hopping, which is a result of static random potential produced by the impurities. The metastable liquid does not contain any quenched disorder. Phenomenological model for the Glass transition has been formulated earlier using similar ideas of movement of free volumes in the liquid [34]. This process of trapping of a particle in the cage [35] formed by its neighbors can be interpreted as being produced by a static random potential and the interaction between currents and density fluctuations which smooth off the ideal transition can be thought of as relaxation via jumps over the almost static potential barriers.

In the present work, however, we see that the numerical solutions of the equations of NFH at very low temperatures show signatures of activated hopping between free energy minima. The crossover seen from a continuous liquid type dynamics to activated dynamics is demonstrated in terms of the time correlations of a state vector $|\Psi^\alpha\rangle$. Our findings here with NFH equations are similar to that of Monte Carlo dynamics or kinetic Ising type models. Analysis of the density distribution obtained from the solution of the NFH equations, identifies a vacancy density for the undercooled system. The vacancy field here does not present a new slow variable since there is no new conservation laws in the system. Dynamic correlations of this vacancy density field $\varrho(\mathbf{x},t)$ are similar to that of the particle density field $\rho(\mathbf{x},t)$. The introduction of the vacancy or void density field $\varrho(\mathbf{x},t)$ in the present work in the last section is reminiscent of similar treatment of the fluctuating hydrodynamic formulation by inclusion of extra slow modes for the supercooled liquid [36–38].

Our primary focus in the present work is on the dynamic behavior of the supercooled liquid in the FEL description. The analysis involves using numerical solutions of the equations of NFH for a set of coarse grained densities. These stochastic partial differential equations have generally been used for constructing field theoretic models for the dynamics of dense liquids. Perturbative treatments of these nonlinear models give rise, at the one loop order, to the MCT of glassy dynamics described above. Complimentary to these continuum models is the molecular dynamics simulation of a small number of particles at high density or low temperature. Simulation studies done using various kinds of equations of motion, like the reversible Newtonian dynamics or stochastic Brownian dynamics, show similar long time relaxation behavior at supercooled densities. Following this approach various microscopic studies over the past decade have now established that the glassy state is characterized by formation of spatiotemporal fluctuations. Atoms in different environments move differently and at any

given time, different regions of the deeply supercooled liquid relax at different rates. The transient spatial fluctuations in the local relaxation behavior have been termed as dynamical heterogeneities of the glassy state [20,39–41]. However, in the ergodic liquid state, the different types of dynamics in different spatial environments hold only for a finite duration. Several studies have indicated that the dynamical heterogeneities are effectively quantified in terms of a dynamic correlation length which can be identified from the study of four point correlation functions [42–46] for the liquid state. The present study of the

time evolution of the coarse grained densities can be extended to compute such higher order correlation functions [46,47] and hence can be useful in the study of dynamical heterogeneities from continuum models.

ACKNOWLEDGMENTS

[1] D. J. Wales, *Energy Landscapes* (Cambridge University Press, Cambridge, New York, 2003).

[2] M. Goldstein, J. Chem. Phys. **51**, 3728 (1969).

[3] T. V. Ramakrishnan and M. Yussouff, Phys. Rev. B **19**, 2775 (1979).

[4] Y. Singh, Phys. Rep. **207**, 351 (1991).

[5] H. Löwen, Phys. Rep. B **237**, 249 (1994).

[6] Y. Singh, J. P. Stoessel, and P. G. Wolynes, Phys. Rev. Lett. **54**, 1059 (1985).

[7] C. Kaur and S. P. Das, Phys. Rev. Lett. **86**, 2062 (2001)

[8] J-P. Hansen and I. R. McDonald, *Theory of Simple Liquids*, 3rd ed. (Academic, London, 2006).

[9] C. Dasgupta, Europhys. Lett. **20**, 131 (1992).

[10] T. Odagaki, T. Yoshidome, T. Tao, and A. Yoshimori, J. Chem. Phys. **117**, 10151 (2002).

[11] S. P. Singh and S. P. Das, J. Phys.: Condens. Matter **19**, 246107 (2007).

[12] P. Chaudhuri, S. Karmakar, C. Dasgupta, H. R. Krishnamurthy, and A. K. Sood, Phys. Rev. Lett. **95**, 248301 (2005).

[13] C. Dasgupta and O. T. Valls, Phys. Rev. E **50**, 3916 (1994).

[14] K. Fuchizaki and K. Kawasaki, J. Phys. Soc. Jpn. **67**, 2158 (1998).

[15] K. Kawasaki, Phys. Rev. **145**, 224 (1966).

[16] B. S. Gupta, S. P. Das, and J.-L. Barrat, Phys. Rev. E **83**, 041506 (2011).

[17] S. P. Singh and S. P. Das, Phys. Rev. E **79**, 031504 (2009).

[18] S. K. Ma and G. F. Mazenko, Phys. Rev. B **11**, 4077 (1975).

[19] S. P. Das and G. F. Mazenko, Phys. Rev. A **34**, 2265 (1986).

[20] S. P. Das, *Statistical Physics of Liquids at Freezing and Beyond* (Cambridge University Press, United Kingdom, 2011).

[21] L. M. Lust, O. T. Valls, and C. Dasgupta, Phys. Rev. E **48**, 1787 (1993).

[22] K. Kim and T. Munakata, Phys. Rev. E **68**, 021502 (2003).

[23] J. D. Bernal, Proc. R. Soc. London A **280**, 299 (1964).

[24] M. Baus and Jean-Louis Colot, J. Phys. C **19**, L135 (1986).

[25] H. Löwen, J. Phys.: Condens. Matter. **2**, 8477 (1990).

[26] C. Bennett, J. Appl. Phys. **43**, 2727 (1972).

[27] D. M. Due and A. D. J. Haymet, J. Chem. Phys. **103**, 2625 (1995); D. M. Due and D. Henderson, *ibid.* **104**, 6742 (1996).

[28] U. Bengtzelius, W. Götze, and A. Sjölander, J. Phys. C **17**, 5915 (1984).

[29] S. P. Das, Rev. Mod. Phys. Rev. **76**, 785 (2004).

[30] D. R. Reichman and P. Charbonneau, J. Stat. Mech. (2005) P05013.

[31] S. P. Das and G. F. Mazenko, Phys. Rev. E **79**, 021504 (2009).

[32] W. Götze and L. Sjögren, Z. Phys. B **65**, 415 (1987).

[33] W. Gőtze and L. Sjögren, Transp. Theory Stat. Phys. **24**, 801 (1995).

[34] G. S. Grest and M. H. Cohen, Adv. Chem. Phys. **48**, 455 (1981).

[35] T. Odagaki and Y. Hiwatari, Phys. Rev. A **41**, 929 (1990).

[36] J. Yeo and G. F. Mazenko, Phys. Rev. E **51**, 5752 (1995); J. Yeo, *ibid.* **52**, 853 (1995).

[37] S. P. Das and R. Schilling, Phys. Rev. E **50**, 1265 (1994).

[38] C. Z. Liu and I. Oppenheim, Physica A **235**, 369 (1997).

[39] M. D. Ediger, Annu. Rev. Phys. Chem. **51**, 99 (2000).

[40] L. Berthier, Physics **4**, 42 (2011).

[41] L. Berthier, G. Biroli, J.-P. Bouchaud, L. Cipelletti, and W. van Saarloos, Eds., *Dynamical Heterogeneities in Glasses, Colloids, and Granular Media* (Oxford University Press, Oxford, 2011).

[42] C. Dasgupta, A. V. Indrani, S. Ramaswamy, and M. K. Phani, Europhys. Lett. **15**, 307 (1991).

[43] C. Donati, J. F. Douglas, W. Kob, S. J. Plimpton, P. H. Poole, and S. C. Glotzer, Phys. Rev. Lett. **80**, 2338 (1998).

[44] W. Kob, C. Donati, S. J. Plimpton, P. H. Poole, and S. C. Glotzer, Phys. Rev. Lett. **79**, 2827 (1997).

[45] L. Berthier and G. Biroli, Rev. Mod. Phys. **83**, 587 (2011).

[46] G. Biroli and J. P. Bouchaud, Europhys. Lett. **67**, 21 (2004).

[47] C. Kaur and S. P. Das, Phys. Rev. Lett. **89**, 085701 (2002).